

Micropower Turbine Structure



ME 495 Autumn 2013

Project Advisor: Dr. Brian Polagye

Submission Date: December 13th, 2013

Team Members:

Clinton Overman
Drew McCullough
Michael Haack
Nam Nguyen

Executive Summary

This report provides a detailed account of our work throughout the quarter to develop a structure capable of accommodating the micropower turbine assembly developed by researchers at the University of Washington to power a customizable instrument package throughout its deployment. It describes all important aspects of the design, manufacturing, and testing of a prototype structure, and includes recommendations regarding the loosening of key constraints.

After generating concepts for such a structure, a couple basic ones prevailed: a three-legged base and a comparable four-legged one. Preliminary analysis showed that the four-legged structure provided significantly more resistance to overturning, but not enough (within the constraint on maximum weight) for a factor of safety much greater than one. Utilization of foils was explored to provide down-force and also to protect infrastructure items and improve flow stability. Computational Fluid Dynamics (CFD) analysis dispelled the expectation that these skirts would provide significant down-force, and later an inverted model, more like a (simple) wing than the first design, was tested for the desired down-force effect. Scale-model flume testing confirmed an important piece of the CFD results: the inverted-skirt design was more resistant to overturning.

The scale models were tested in much lower flow velocities than the prescribed design velocity of 2.5 m/s and at lower velocities even than the maximum flume velocity (0.7 m/s), at which we conducted the CFD analysis. Nonetheless, we correlated the CFD results to the test results by assuming the coefficients of lift and drag from CFD to be the same as at the (lower) tested velocities. We then made the same assumption in scaling the CFD and test results, which mostly agreed with each other, to our design case of 2.5 m/s and for the full-scale design. Based on this analysis the better-performing inverted structure is near to strictly satisfying the design requirements at full-scale *but without significant safety margin*: to have a factor of safety against overturning of two, for example, would require significantly more ballast.

Some additional CFD testing may be required to establish its reliability for our purposes, at parameters more similar to those of our flume tests. From here there are two basic and mostly complimentary ways to proceed: 1) explore new designs and features for reducing drag and generating down-force, and 2) significantly increase the ballast, perhaps by up to 50%, and deal with the challenges associated with a heavier structure. The first is probably insufficient by itself, and even if it were feasible it would require extensive modeling (and maybe testing) and perhaps over numerous design iterations. Thus our recommendation is to increase ballast; our test results, in place of further extensive modeling and analysis, can be used to determine a refined estimate of just how much additional ballast would be required. Depending on this amount and the extent to which it would introduce a hazard to safety and otherwise encumber deployment and recovery, some effort could be made to reduce the more significant contributors to total overturning moment.

Table of Contents

Problem Definition.....	1
Motivations.....	2
Current Technology.....	2
Concept Generation/Selection.....	2
Scale Model CFD.....	4
Flume Test Scale Models.....	6
Model Manufacturing.....	8
Flume Test.....	9
Test Results and Analysis.....	11
Design Recommendations.....	14
Risk and Liability.....	16
Ethical Issues.....	16
Consideration of Impacts on Society.....	17
Consideration of Impacts on Environment.....	17
Future Work.....	18
Appendix.....	19

Problem Definition and Constraints

The goal of this project is to design a structure to support a microturbine, generator, and instrument package that will not overturn in tidal currents. Constraints were placed on the structure design in order to make deployments practical and possible. Before getting into too much detail about the constraints it is helpful to breakdown the main sections of the system that will be discussed throughout the report. Figure 1 below shows a full scale design of the structure with the main components indicated.

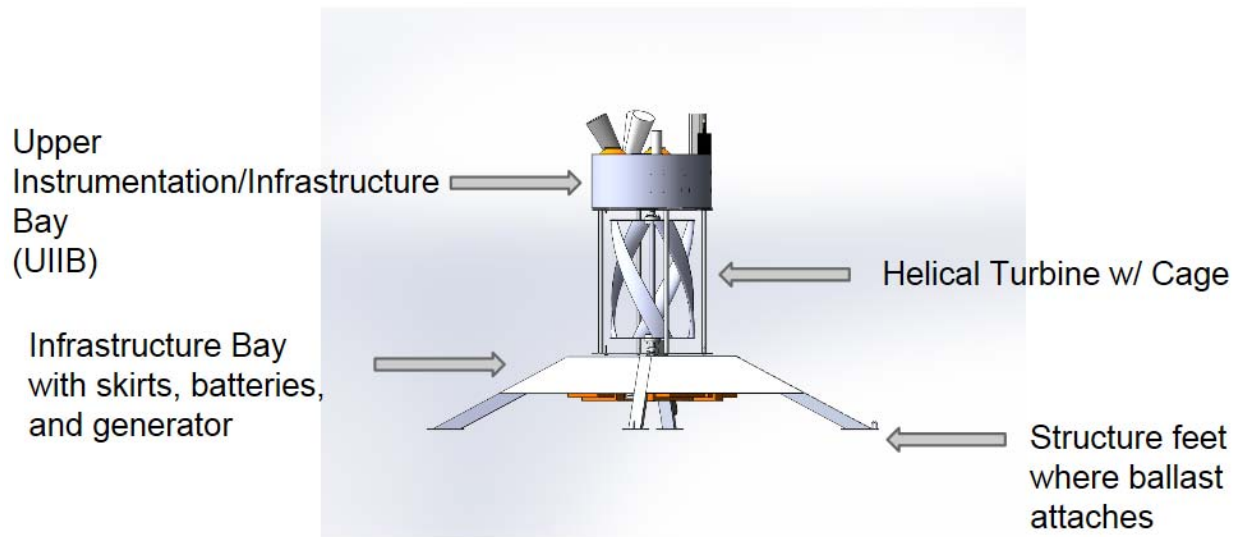


Figure 1. Breakdown of the main structural elements

The height of the entire structure (base, turbine, instrumentation package) can be no greater than 3 meters (9.8 ft). Likewise, the widest part of the entire structure cannot exceed 3 meters (9.8 ft). Clearance from the seabed is also constrained. The minimum distance between the ground and the bottom of the turbine plate is 60 cm (2 ft) and the minimum distance between the ground and the lowest part of the Lower Infrastructure/Instrumentation Bay (LIIB) is 30 cm (1 ft). The reasoning behind these minimum clearances is to ensure nothing but the legs will make contact with the seabed, even in the case of the structure landing on a rock. If the clearances are not great enough, the potential of the underside of the structure landing on a rock increases. Landing in this position would significantly increase the risk of overturning and could damage equipment in the LIIB. The budget for the full size design (all materials excluding lead and infrastructure elements) is \$2500. Additionally, the weight in air of the entire assembly cannot exceed 1100 kg (2500 lbs.) This weight was chosen as a safety precaution for those who would be deploying the generation and instrumentation package from the working deck of a research vessel.

In order to consider the design acceptable, the structure must be able to resist tipping in what are considered extreme conditions. The two conditions are withstanding currents up to 2.5 m/s

(8.2 ft/s) in the most unfavorable direction, and to have the structure start at a 5 degree incline to simulate an uneven seabed.

Project Motivations

Currently, the most common source of power for marine instruments is the battery. While the battery does provide a steady source of power to the instruments, it is a finite energy source which limits the duration of the package's deployment. Constantly replacing these batteries is not only expensive but wasteful. On the other hand there is the possibility of a direct source of power by way of cables from shore to the structure. The research team would look to deploy the structure quite a distance offshore and at nearly \$1 million per mile, the cost is a main deterrent for this option. With current power methods being less than desirable, a microturbine and generator package that can generate continuous power becomes attractive. The turbine, generator, and instrument package require a large structure to not only support them, but keep them from toppling over as well. The current structure that is deployed for autonomous instrumentation (an Oceanscience, Ltd. Sea Spider) would easily tip over in the tidal currents with all of these items affixed to it. Thus, this is the motivation for the design of a new and improved structure.

Current Technology

Current designs that exist for support structures for marine studies include the Sea Spider and the Barnacle, both of which are made by a company called Oceanscience, Ltd. These structures employ fiberglass frames to support research equipment and battery packs for power. The essence of the Barnacle design is not adaptable for our purposes, and the Sea Spider is too small to support the turbine. However, both can provide inspiration for our eventual design; in particular, the basic idea of the Sea Spider is one that will be used. The key structural feature of this design is a relatively low and wide (tripodal) base. Unlike a basic tripod the Sea Spider has a central platform for versatile mounting of instruments, sensors, etc. Also, the legs are not constructed out of prefabricated structural members (e.g. tubing or square beam), and instead are broader and therefore have more mounting area.

Concept Generation/Selection

Initial design concept generation was inspired by the design of the Sea Spider. Generally, the first designs consisted of a flat plate to support the turbine with support legs extending down to the ground and skirts running between the legs to protect infrastructure items such as the generator and batteries as can be seen in Figure 2. In addition to added protection, the skirts were also initially thought to provide down-force that would help to resist tipping.

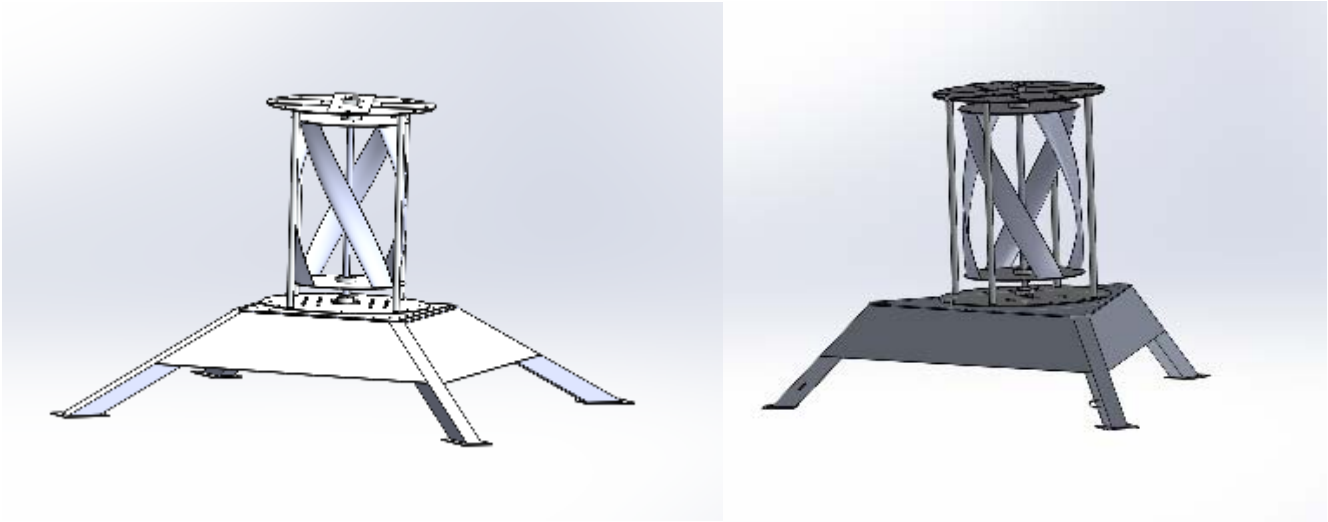


Figure 2. Initial designs, four and three legged with standard skirts

The four-leg model offers a significant advantage of being able to bare more weight, as package weight would be distributed among four legs instead of three, but this alone was not enough to make the four-leg an outright winner. The big concern with using four legs is that only three legs are guaranteed to make contact with the seabed at any given moment, unless the legs can incorporate some flexibility in their contact point. It was desired to keep the design as simple and reliable as possible, so trying to design for flexibility wasn't a good option. In the end it was decided to consider the worst-case scenario of uneven ground and the current in the right direction, which would cause the structure to start tipping until that leg makes contact to the seabed and lifts up another. These effects would be considering when comparing tipping potential between the two models, and be most important in choosing the final design.

Preliminary drag and tipping analysis for each structure was performed analytically, and revealed that the four legged structure was far superior to the three legged structure due to its longer moment-arm from center of mass to the fulcrum at the outer edges of two back feet. It had to be decided if the advantage in tipping outweighed concerns about the stability of the four legged structure on an uneven sea bed. When weighing the possibilities for a worst case scenario of uneven ground at 10 degrees, it was concluded that the difference in resisting moment was small considering the same may happen if a leg was set down on a rock or instability that would produce the same overall tilt angle. Furthermore, the tipping back and forth would happen as the tide gently changed velocity, so the dynamic nature of the tip is not expected to be a risk to the overall stability. From here on, design focused on the superior four-leg design.

The models were put through preliminary CFD analysis using ANSYS Workbench and its Fluent solver. After trials of several simplified models consisting of simplified pyramids for the base and a block on top to simulate the turbine, the tests revealed that the initially proposed "semi foil" design actually produced vertical lift rather than downward force. After reviewing CFD

velocity plots it was concluded the structure was functioning somewhat as a crude wing. It was then proposed to invert the skirts on the bottom of the structure to try and reverse the effects of the flow around the object to create down-force rather than lift. More will be said on the CFD testing process in the next section.

Scale Model CFD

To compare the inverted and standard skirt concepts, a flume test was arranged to experimentally test the skirt effects on the tipping moment of $\frac{1}{8}$ scale models. Prior to flume testing a CFD analysis was performed on the scale model base structures using Fluent within Ansys Workbench. The purpose of the CFD analysis was to model the forces on the base structures and to find the coefficients of lift and drag.

In all cases that were tested, the setups in Fluent were very similar. In the analysis the fluid was modeled to be seawater with a density of 1025 kg/m^3 (63.9 lb/ft^3) and a viscosity 0.0011 kg/m-s . Additionally, a k- ω turbulence closure was utilized. The area of the modeled flow was three characteristic lengths upstream of the models, three above and to the sides, and 10 characteristic lengths of the model downstream. This region was designed to be large enough to capture all of the velocity and pressure changes due to flow interaction with the models. The boundary conditions for the region define how the flow behaves. Both the model structure and the floor have wall boundary conditions which equates to a no-slip condition. The upstream surface has a velocity-inlet boundary condition set at 0.7 m/s and the downstream wall is a pressure-outlet. For the two side walls and the top of the region the desired boundary condition of mirror symmetry, which is a symmetry boundary condition in Fluent. The boundary conditions were the same for all simulations, and after meshing, each case had approximately 4 million nodes with low element skewness (an average skewness of less than 0.9.)

The $\frac{1}{8}$ scale base structures were tilted to the required angle of 5 degrees for simulation. Below in Figure 3 the CFD test models can be seen with the standard design on the left and the inverted on the right.

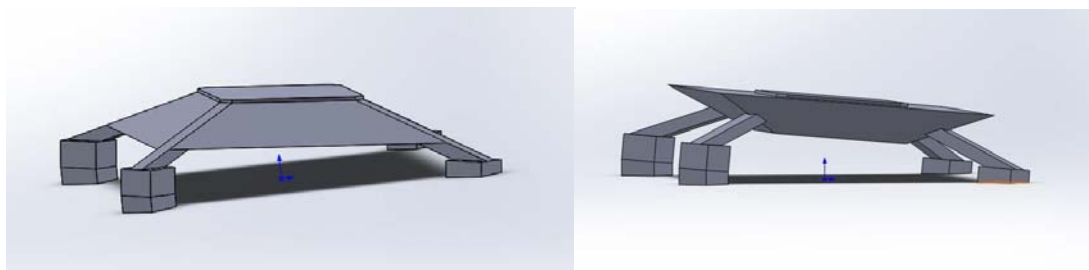


Figure 3. Models used in CFD analysis

Figure 4 shows the velocity contours with the results of the CFD simulation run at 0.7 m/s (2.3 ft/s) with the standard base structure. It can be seen that the fluid is accelerated over the top surface of the model which creates a low pressure zone, resulting in positive, vertical lift.

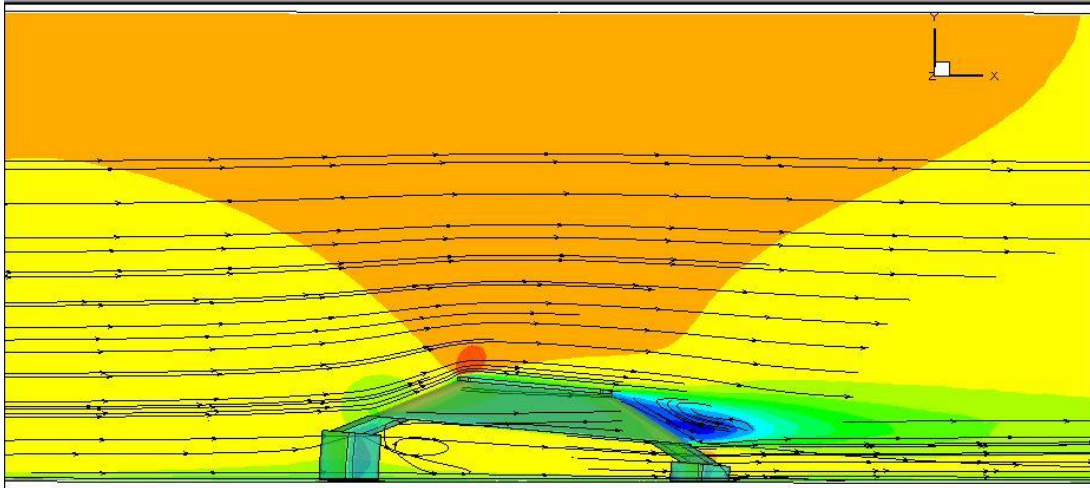


Figure 4. Velocity heat map of flow at 0.7 m/s (2.3 ft/s) with standard model

The inverted skirt model and an inverted skirt with a plate representative of the drag on a turbine were also analyzed. Understanding the effects of the increased flow blockage on the lift coefficient is important because a decrease in the lift force on the structure is very important in terms of the induced tipping moment. From previous CFD simulations it was seen that the decrease in lift on the standard model when tested with a block above was very minimal compared to that of the inverted model with a block above and is therefore not considered here. Below in Figure 5 a side by side comparison of the flow around the inverted and inverted with plate designs can be seen. Notice the large pockets of low velocity flow created by the addition of the plate as compared to the structure without a plate.

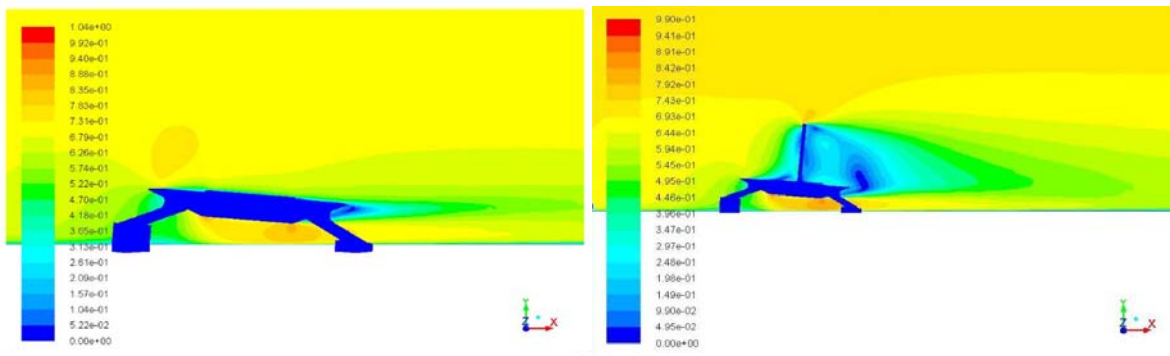


Figure 5. Velocity profiles of inverted and inverted with plate

The results from the CFD analysis are below in Table 1. Comparing the two inverted structure tests, it is easy to see how the lift on the structure is very sensitive to the additional blockage created by the plate. The lift coefficient, which is defined below in Equation 1, dropped from 0.5 to 0.05 and the lift force decreased from 3.8 N (.85 lb) to 0.5 N (.11 lb,) which is an 86% decrease in lift force. The sensitivity of the lift coefficient of the inverted structure to flow blockage is an important aspect of the design moving forward.

(1)

$$C_l = \frac{L}{\frac{1}{2}\rho v^2 A}$$

L – lift force, *ρ* – fluid density, *v* – fluid velocity, *A* – projected surface area

Table 1. Pre-Flume CFD Results

	Standard	Inverted	Inverted w/ Plate
Coefficient Of Drag	0.5	0.7	-
Drag Force	3.3 N (.7 lb)	4.9 N (1.1 lb)	-
Coefficient Of Lift	0.7	0.5	.05
Lift Force	5.1 N (1.1 lb)	3.8 N (.9 lb)	.5 N (.1 lb)

Flume Test Scale Models

Two 1/8 scale models were designed and constructed to be tested in the flume. One model would utilize a standard skirt design and the other would have the inverted skirt. Below in Figure 6 and Figure 7 isometric and side views are shown of the standard and inverted models respectively.



Figure 6. Standard Skirt Scale Model

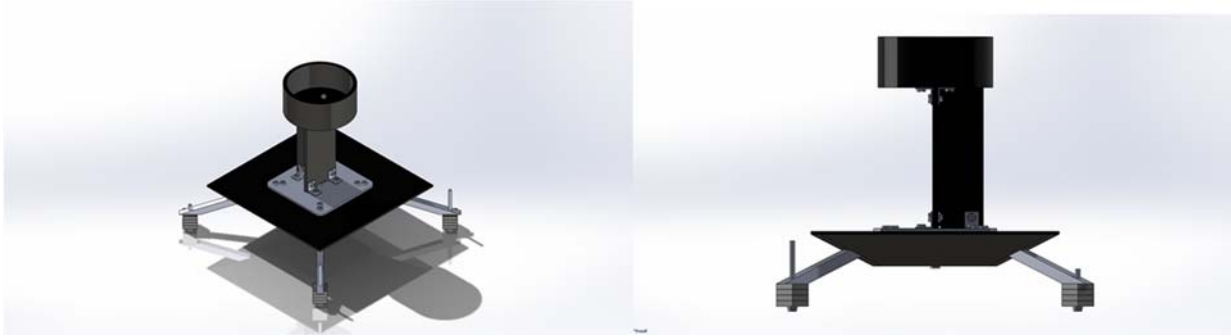


Figure 7. Inverted Skirt Scale Model

The ballast attached to the feet are 1x1x.25 in. bars of steel (four pieces each foot) and are attached to the structure legs via 1 ½ in. bolts in the back or 3 in. bolts in the front feet. By placing much longer bolts in the front feet, the model was capable of adjusting angle in the flume by adjusting the height of the front. The ½ x ½ in. square legs and ¼ in. thick top plates were all made of 6061 aluminum to stay consistent with the materials that would be used on a full scale design. In order to reduce the weight of the components so that the model weight would scale near 1/8 as well, ABS plastic was chosen for the skirts, turbine plate, turbine plate support rib, and UIIB.

A single plate was used to represent the turbine on the model because the time and resources were not available to produce a functioning turbine. However, the area of the flat plate was scaled so that the drag force it produced matches that of a turbine. Using the known coefficient of drag of a plate and the coefficient of drag of the turbine, the frontal area of the plate could be calculated. The height of the turbine plate is 15.9 cm (6.25 in.) at the 1/8 scale, and using the equation of drag seen below and drag coefficients of 2 and 1.1 for the plate and turbine, respectively, produced a plate width of 7.2 cm (2.82 in.)

$$(2) \quad F = \frac{1}{2} \rho v^2 C_d A$$

F – drag force, *ρ* – fluid density, *v* – fluid velocity, *C* – coefficient of drag, *A* – projected area

Inside the enclosed skirt area, a 2 ½ in long bolt runs through the top plate so that additional ballast could be added or removed, as well as to secure the bottom plate which can be seen in Figure 8 of both models. This enclosed area was not designed to be airtight so that water would enter when submerged in the flume. Otherwise the whole volume contained within the skirts would have a large buoyant force detrimental to stability.



Figure 8. Section views showing internal bolt for ballast and bottom plates

A box was drawn to the exact 1/8 scale dimensions of the structural size constraints. Placing the scale models within this box, as seen in Figure 9, provides a quick visual check to ensure that the size constraints are being satisfied. Figure 9 confirms that the models satisfy the project size constraints.

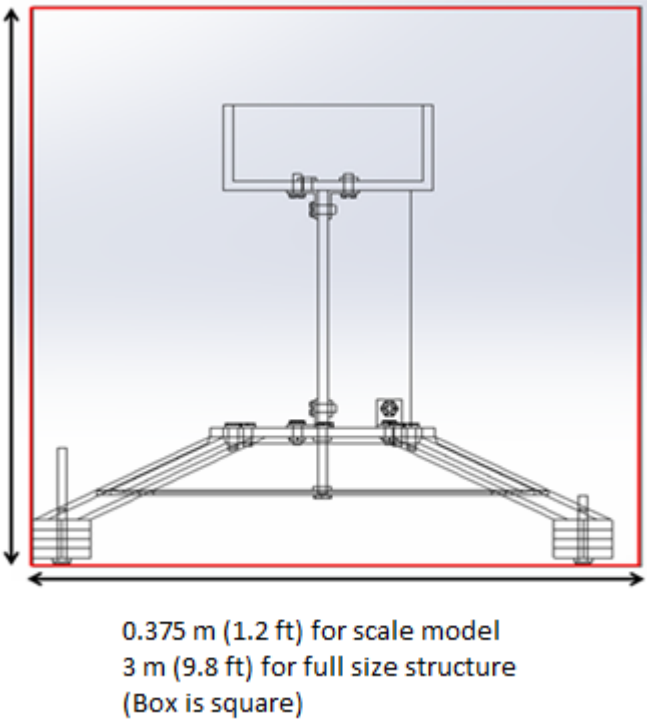


Figure 9. 1/8 scale size constraints enveloping scale model

Model Manufacturing

The manufacturing process for the models can simply be broken down into the fabrication of the individual components and assembly. The aluminum legs and top plate were cut using a band saw and then machined using a two-axis mill to the specified model dimensions. Holes were then drilled through the plate and feet so that they could be assembled together using 10-32 1/2

in bolts and nuts. Additionally, holes were drilled into the top plate so that the turbine plate and support rib could be affixed to it. The turbine plate and support rib were cut down and then machined out of ¼ in. thick ABS sheets. Once again holes were drilled in these plates, as well as the 12.7 cm (5 in.) diameter scale-UIIB, so these components could be bolted via brackets to the top plate and each other. It should be noted that only one turbine plate, support rib, and UIIB were constructed because they are identical for each model and thus could be transferred between the two base structures during testing. Lastly, the skirts and bottom plates were measured and cut out of 1/8 in. thick ABS sheets using a sheet metal cutter and a Dremmel cutting tool.

Upon completion of the manufacturing stage, assembly of the models began. The first step was to bolt the legs to the top plate to create a frame for attaching the skirts. Using Loctite Marine Epoxy the skirts of the standard design were glued in place quickly and without issue. On the other hand, the inverted design skirt were tricky to assemble because of the small contact surface between the legs and skirts. In appendix A.1 there is an image of the skirts being held in place with weights while the epoxy sets up. The support rib was then epoxied to the back of the turbine plate and once the epoxy finished setting up the UIIB were bolted on and the models were ready for testing. Images of the completed structures can be found in appendix A.2 as well.

Flume Test

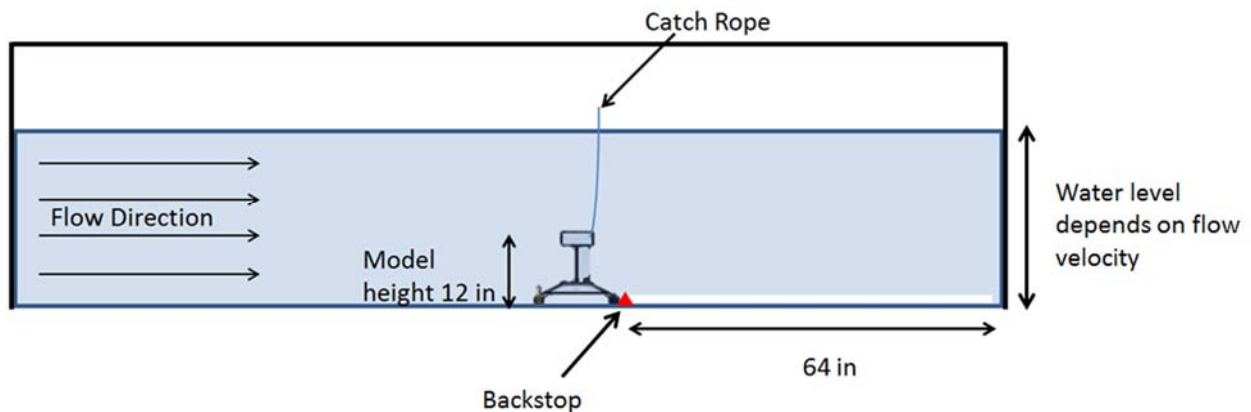


Figure 10. Schematic of the flume test with the standard model (Side view)

To corroborate our CFD results and to compare our different skirt designs, flume tests of our models were conducted. The flume in the Aeronautics and Astronautics building was used to carry out the tests (see the schematic above). The following is a list of each test case:

- Test Case 1: Standard model, 0 degree incline, 200 g (.44 lb) ballast in skirt
- Test Case 2: Standard model, 7.5 degree incline, 200 g (.44 lb) ballast in skirt
- Test Case 3: Inverted model, 0 degree incline, no ballast in skirt
- Test Case 4: Inverted model, 7.5 degree incline, no ballast in skirt

Three trials at were carried out each test case consecutively to avoid frequent adjustments of the testing setup. Figure 11 below shows Test Case 1 (TC1) underwater in the flume.

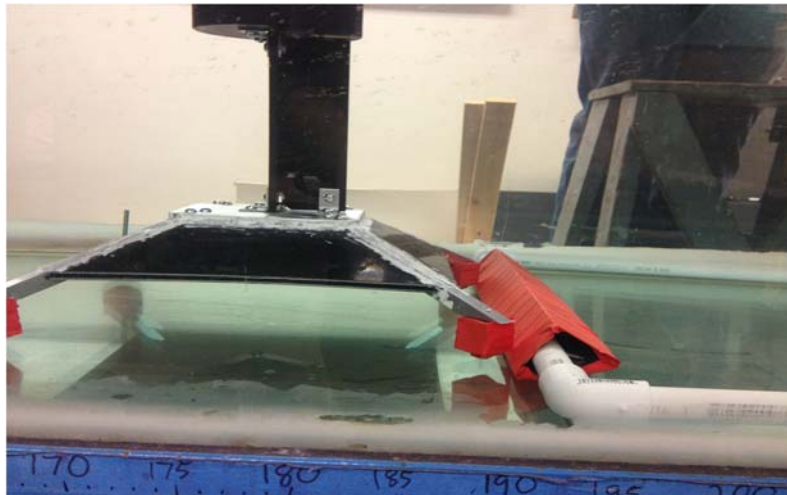


Figure 11. Feet against backstop in flume

Flow passes from left to right. The triangular backstop was made from sheet metal and wrapped in vinyl tape. As shown in the above picture, the back corners of the external ballast blocks, which were also wrapped in vinyl tape, rotated about the front face of the backstop at a fulcrum line several millimeters above the bottom of the flume. The 2.54 cm (1 in) dia. PVC-pipe frame extended to the back of the flume and resisted translation. At the very top of the model attaches a catch rope (not pictured,) which was used to secure and recover the model at the onset of tipping.

Velocities for each of the 3 trials within each test case agree very closely with one another, so listed below in Table 2 is a single Velocity at Onset of Tipping (VOT) for each test case.

Table 2. Flume test results

Test Case	Velocity at Onset of Tipping (VOT), m/s
Standard model, 0 degree incline, 200 g ballast in skirt	0.66 (2.2 ft/s)
7.5 degree incline, 200 g ballast in skirt	0.52 (1.7 ft/s)
Inverted model, 0 degree incline, no ballast in skirt	0.67 (2.2 ft/s)
Inverted model, 7.5 degree incline, no ballast in skirt	0.50 (1.6 ft/s)

The test procedure was straightforward. Each trial was conducted by placing the model in the flume and gradually increasing the velocity until the model tipped, recording this (maximum) velocity as VOT. These velocities are the important result of our testing, and fortunately they agree with each other and make physical sense.

Test Results and Analysis

One of the primary goals of testing was to verify our CFD results. In some way this was primary even to comparing the performance of the models, since with strong evidence that the CFD results are reliable, those very same results could be used directly to compare models, and any future iterations of those or other models could be analyzed with CFD. Our basic methodology for corroborating the CFD was to identify a quantity (or quantities) that could be obtained independently both experimentally and from CFD results, and then to compare the quantity as predicted by the CFD to the quantity as measured. This quantity is the threshold tipping moment, and will be defined as it shows up both experimentally and from the CFD.

The threshold tipping moment -- the moment at which the model just begins to tip -- is exactly equal to the maximum resisting moment of the model, which is designated as the "Adjusted Resisting Moment" (ARM). The ARM is an actual physical quantity that can be determined for each model, and therefore is subject only to measurement uncertainties. The "Predicted Tipping Moment" (PTM) is equal to the tipping moment predicted from the CFD for particular conditions (flow velocity, model type, etc.). For a sample PTM calculation, see Appendix A.5. Every ARM is calculated as an adjustment of the resisting moment of the corresponding base model -- that is, corresponding to the angle of inclination -- where the base model is the non-inverted design without any kind of ballast, external or internal. (For details of the static tipping testing and tabulated results, see Appendix A.3). This adjusted resisting moment, for each model, is a function only of properties of the model (geometry and mass distribution) and therefore is also a property that does not vary with test conditions. The ARM is the maximum tipping moment the model could possibly resist, so at the point of tipping the ARM is also equal to the tipping moment induced by the particular flow velocity; this equality is what establishes a meaningful link between prediction and experiment. So by recording the velocity at onset of tipping (VOT), which for all test cases was within 0.2 m/s (.66 ft/s) of our CFD velocity of 0.7 m/s (2.3 ft/s,) a corresponding predicted tipping moment (PTM) was calculated -- in other words, the value of the moment which the CFD predicts for that particular velocity and test setup. Clearly if the prediction method were perfectly accurate, it would predict a tipping moment exactly equal to the actual tipping moment (which at the point of tipping is exactly equal to the ARM). So our measure of accuracy of the CFD is specified by the closeness of the PTM to the ARM.

The CFD drag assessment was conducted at the maximum flume velocity of 0.7 m/s (2.3 ft/s,) so the flume tests were planned to run at the same velocity. But the test is binary--a model either tips or does not tip at some velocity up to the maximum. In order to extract meaningful

information from every test and to avoid making dozens of ballast adjustments, all four setups were under-ballasted so that the threshold tipping velocity, or velocity at tipping (VOT) for each setup could be determined. Again, from these velocities, the PTM was (re)calculated. See Table 3 below for the PTMs and ARMs for each setup.

Table 3. Test analysis results

Case (test conditions and model #)	PTM (N-m)	ARM (N-m)	% Error	% Contribution of CFD Results to PTM
Standard model, 0 degree incline, 200 g ballast in skirt	2.1	2.1	0	35
7.5 degree incline, 200 g ballast in skirt	2.3	2	15	60
Inverted model, 0 degree incline, no ballast in skirt	1.8	1.8	0	60
Inverted model, 7.5 degree incline, no ballast in skirt	2.0	1.7	18	20

The agreement between PTM and the corresponding ARM is relatively strong, especially for the two non-inclined test cases. Moreover, the uncertainty associated with each ARM value is relatively small. Each value consists of two parts, one experimental (from the static tipping test) and one analytical (the correction for ballast), and both are known with reasonably high accuracy (approximately <5%). Still, for several reasons the results are somewhat inconclusive.

First, there is a relatively high degree of uncertainty associated with the PTM values. Each PTM value is the sum of several moments, and two of those moments come directly from the CFD and are fairly uncertain due, to the limited amount of CFD data. Three major CFD analyses were conducted, one for the non-inverted model and two for the inverted model, all at 5 degrees incline. For the non-inverted model there are only results for just the base without the turbine plate or upper IIB. The lift force predicted from this analysis is therefore unrealistically high since pressures above the base are relatively lower. This is probably why our initial predicted weight was high (ballast had to be significantly reduced to get the model to tip). Since the models were not tested at 5 degrees in the flume, in calculating our PTMs assumptions had to be made about how the changes in angle affected our lift and drag forces on the base. Also, in a couple cases assumptions had to be made about where exactly on the base the lift and drag forces acted since centers of pressures had not been obtained from the CFD. The net effect of all these assumptions, which in every case could not be fully justified, is an error in PTM value in the range of at least 10-30%, depending in each test case on the number of assumptions required to compute the corresponding PTM. One way to improve our estimation of uncertainty would be to set up a spreadsheet to conduct a sensitivity analysis, thereby gauging the effect on PTM values of changes in our assumed values of lift and drag forces and their respective moment arms.

There is at least one other reason to be cautious about taking the results at face value and assume a high accuracy of prediction. Insofar as anything was corroborated, what was actually corroborated (directly) was the combination CFD-Analytical (CFD-A) results, so called because CFD was only performed on the base structure and therefore had to account for the other parts analytically (turbine and upper IIB). And in fact the contribution of the analytical parts to the PTM is significant (much larger than the CFD contribution when lift on the base is relatively small), in which case roughly the same absolute error is being associated with a much smaller quantity, resulting in a much larger percent error (see Table 3 above for percent contribution of CFD parts to PTM). This could be accounted for, roughly, by assuming a certain error for the analytical component of the PTM and attributing the remainder of the error to the CFD component. In test cases 2 and 3 it would result roughly in a doubling of the error estimation, and in cases 1 and 4 it would go up several-fold. (It is somewhat a coincidence and somewhat the results of biased assumptions that in cases 1 and 3 there is no apparent error; in fact there probably is some non-trivial error, and it would be those errors that would get multiplied by the aforementioned factors.) CFD analysis at conditions more similar to the test conditions would be the easiest way to corroborate the CFD analysis without doing extensive (additional) flume testing.

Another important consideration is what the test results tell us about the full-size model. Using the same coefficients of lift and drag from the CFD and scaling areas, the full-size model would require a total weight (in water) of about 45.4 kg (100 lbs), corresponding for our model to a total weight of approximately 113.4 kg (250 lbs) in air. Because our thicknesses did not scale to $\frac{1}{8}$, our model volume is relatively higher and therefore over predicts the total weight in air by about 20-25%. If the coefficients of lift and drag remained the same at flows of 2.5 m/s (8.2 ft/s), the total resisting moment would need to be about 14 times higher, corresponding to a weight in water of about 635 kg (1400 lbs), restricting the displacement of the model to 500 kg (1100 lbs) to remain within the 1100 kg (2500 lb) weight limit in air..

The above values are *threshold* values (i.e., stability is marginal). To maintain a comfortable factor of safety, significantly more ballast would be needed. See Table 4 below for the breakdown of tipping moment by component.

Table 4. Breakdown of tipping moments (given by component as percent of total PTM)

Test Case	Upper IIB (%)	Turbine Plate (%)	Base (from drag) (%)	Base (from lift) (%)
Standard model, 0 degree incline, 200 g ballast in skirt	26	40	5	29
7.5 degree incline, 200 g ballast in skirt	16	25	17	42
Inverted model, 0 degree incline, no ballast in skirt	30	48	9	13
Inverted model, 7.5 degree incline, no ballast in skirt	17	27	31	25
Case Average	22	35	16	27

Design Recommendations

The decision on whether to go with the inverted plates or the standard plates is inconclusive. Although the design with the inverted plate performs better than the standard plates, the results are not favorable enough to go forward with a full scale model. The recommended path going forward would be to look into increasing the ballast to stabilize the structure while keeping the number of legs at four. Instead of using plates/skirts in the lower IIB to try to create a negative vertical lift force, a more practical approach (both in performance and in manufacturability) might be to simply weld a cylinder onto the lower plate of the turbine to protect the generator and focus on minimizing drag.

The upper instrumentation/infrastructure bay required special attention in the layout due to the instruments' sensitivity to interference. A list of all the components in the upper IIB can be found in appendix section A.4. The Doppler profiler became the most challenging to place because it has three transducers that points out radially that needs to be clear of any obstruction along its projected path (~ 2 degree expansion of acoustic beams). Because of its complicated nature, the Doppler profiler was the first instrument to go into the layout and everything else would be arranged accordingly (as displayed in Figure 12). Most of the instruments are attached to the cylinder wall using some sort of strap or clamp to hold them in place. The thing to note in the UIIB is the line routing for the recovery buoys. The line ties off from the pick point in the middle of the upper IIB and feeds into the vertical line canisters. The line then comes out of the canisters and runs through the top of the buoys. The line would then be tied to a shackle which is attached to the acoustic release that sits directly underneath the buoys to hold the buoys in place.

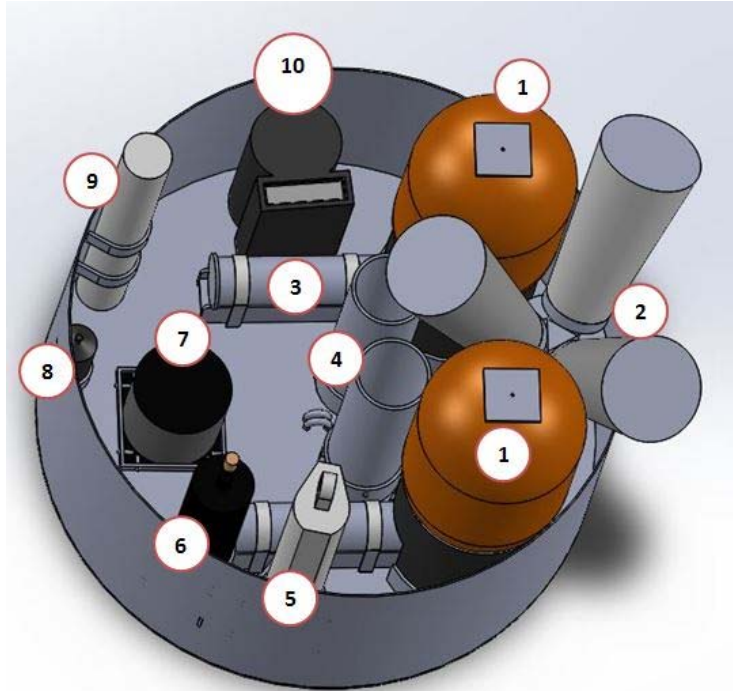


Figure 12. Upper Instrumentation/Infrastructure Bay (Doppler profiler beams shown for reference)-Instrument labels in A.3

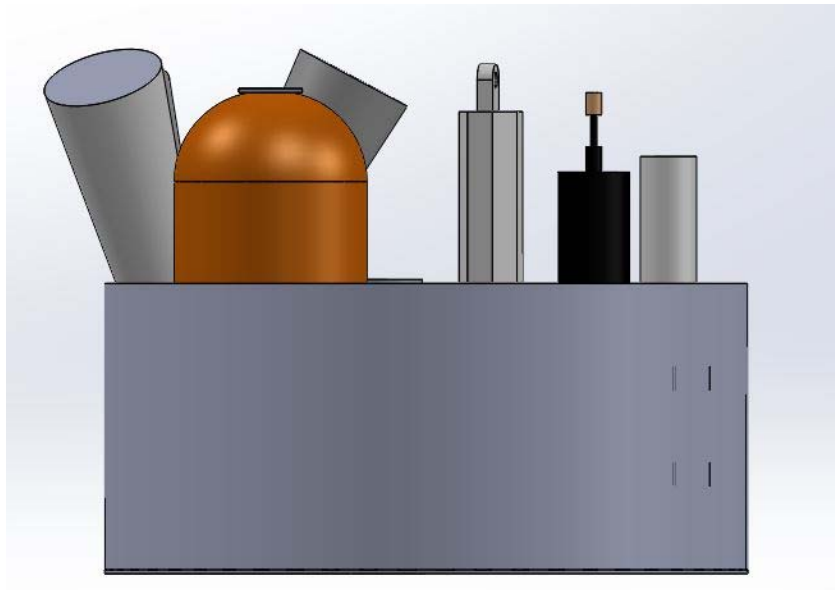


Figure 13. Side view of UIIB

Risk and Liability

With such a large and heavy unit, the main risk involved with the hydrokinetic turbine package would most likely occur during transportation and deployment. With the package possibly spanning up to 3 m (9.8 ft) wide and weighing up to 1100 kg (2500 lbs,) maneuvering the entire unit can be extremely dangerous for the unit and anybody around it. With something that large and heavy, if it begins to swing while being lifted by a crane, it could be rather difficult to regain control and stabilize the unit. To prevent the package from swinging out of control during deployment, there will be two eye bolts attached to the legs where a tag line can loop through. As the crane picks up the unit, operators on either side of the unit can pull on the cable outwards to help stabilize it while it is in midair.

Another risk to consider is the possibility of a failure during recovery. If the acoustic release doesn't work when needed, it would not be able to release the shackle holding the buoy in place. In order to offset that risk, the use of a second buoy/acoustic release system is recommended. It is obviously a redundancy in the design, but without a backup plan, the structure may be impossible to recover should the first system fail.

An important liability to consider is the protection of the instruments used. All of the instruments that are expected to be used in the deployments are rather expensive and sensitive. The potential in damaging the instruments cannot be ignored. Extra caution would have to be taken to design the layout of the upper instrumentation infrastructure bay to ensure that the instruments do not interfere with each other, but also to make sure that all the instruments are secured properly. Additionally, overturning of the structure risks damaging the instruments and other expensive system elements such as the turbine.

Ethical Issues

With every new design, the consideration of violating an existing patent must be visited. The foundation of any of the designs came from the design of the Sea Spider. Although the Sea Spider was used as the starting point, all of the designs generated during the course of the project are unique enough to not be in risk of violating existing patents. The legs of the final design should be enough to differentiate itself from the Sea Spider (four straight legs opposed to three bent legs on the Sea Spider).

To restrain from spending an excess amount of money on the structure once the design is finalized, careful analysis will need to be done to minimize the weight of the structure without breaching the safety factor deemed reasonable for the structure. When presenting the final design to the funder of the project, that person(s) may look to decrease the amount or quality of the materials in the design in order to save on cost. Should this happen, keeping the importance of the safety of factor in mind is critical.

Consideration of Impact on Society

If the microturbine system is deployed and functions properly then it has the potential to make an impact on society. From a research standpoint, the possibility of continuous power greatly increases the duration of monitoring studies in the ocean. Marine life to ocean conditions will all be able to be monitored using the instrument package in the UIIB, information which is useful and a variety of applications. One such application is monitoring marine life traffic as a study to check the viability of placing commercial grade turbines in tidal channels for the generation of electricity. If this microturbine system can help collect the needed data to push for the implementation of these commercial sized turbines, then many surrounding areas have the potential to be powered by a green energy source.

Consideration of Impact on the Environment

The environmental impact of the hydrokinetic turbine system is something that must be seriously considered before a prototype is tested in the field. Any sort of negative impact, such as habitat destruction, pollution, or endangering marine life, comes with ethical and potentially legal implications. Therefore, it is our job as engineers to try to minimize or prevent any potential environmental impacts. When considering our system, looking at the impact of the turbine, structure, and attachable packages separately helps to break down the overall impact on the environment.

Looking at the turbine first, the major concern is whether or not the spinning blades put sea life at risk. As of right now research is still being done to investigate if marine life will be attracted to a spinning turbine or will avoid it. If the latter is found to be true, then it would be safe to assume that a turbine would pose little danger. However, if marine life is attracted to the turbine, then the turbine does potentially create a dangerous situation. Considering the relatively small size of the turbine, low angular velocity of the blades, and low momentum at a current flow rate of 2.5 m/s (8.2 ft/s,) the turbine wouldn't pose much risk to marine life even if it were to be struck by a blade. Thus, the environmental impact of the turbine would be very low.

The support structure of the turbine should have very little impact on the surrounding environment other than where the feet touch the ground. The structure will be very heavy (approx. 1100 kg (2500 lbs)) and any living thing that is underneath the feet when it touches down will surely be crushed. However, with the four feet having a footprint of .077 m² (120 in²,) the probability of landing on any marine life or sensitive habitat will be extremely low. Additionally, the zone where the turbine structure is to be placed will be scouted out ahead of time to locate a prime deployment site. The structure itself will be made from aluminum with stainless steel fasteners, both of which can be recycled at the end of the structures lifecycle.

Lastly, there are the various instruments and infrastructure elements to consider. Within this range of items are the large lead-acid sea batteries. The chemicals contained inside the battery can be harmful to marine life as well as the surrounding environment if they are leaked. The

batteries that are used as a part of our hydrokinetic turbine system are designed for use in marine environments so that they do not leak, even at depths of up to 1100 m (3600 ft.)

After careful consideration, it has been found that the turbine system has a very small impact on the environment around it and should be safe to deploy. As always the pursuit of minimal environmental impact should be continued.

Future Work (Project Continuation)

Before a full scale design can be finalized and prototyped there is still work to be done. It is recommended that an extensive CFD analysis be performed on the models systematically. Breaking the model down into base structure, turbine region, and UIIB and analyzing each individually will help future engineers to understand what each component contributes to the tipping moment. Additionally, the models should be analyzed as a whole, adding and removing components to see what effects the interacting flows have on the models performance. An example of this would be comparing how the inverted base performs with the turbine plate vs. without it. Running these tests at a variety of velocities and angles will help button down the coefficients of lift and drag as well. Along with the CFD, valuable information could be gained from modeling the actual turbine blockage at varying velocities and comparing this blockage to that of an equivalent drag plate.

Another avenue to go down would be to look into alternative ways to anchor the structure to the ground besides trying to create negative lift or relying purely on attached ballast. One possible solution could be to deploy a large ballast package separately from the structure that the structure could then lock into when it is deployed.

Further research could be done into other foil designs that can create negative lift while also minimizing the amount of drag. The inverted skirts in the flume test were able to bring the lift down to nearly nothing but still produced a large drag force that contributes to the tipping moment of the system.

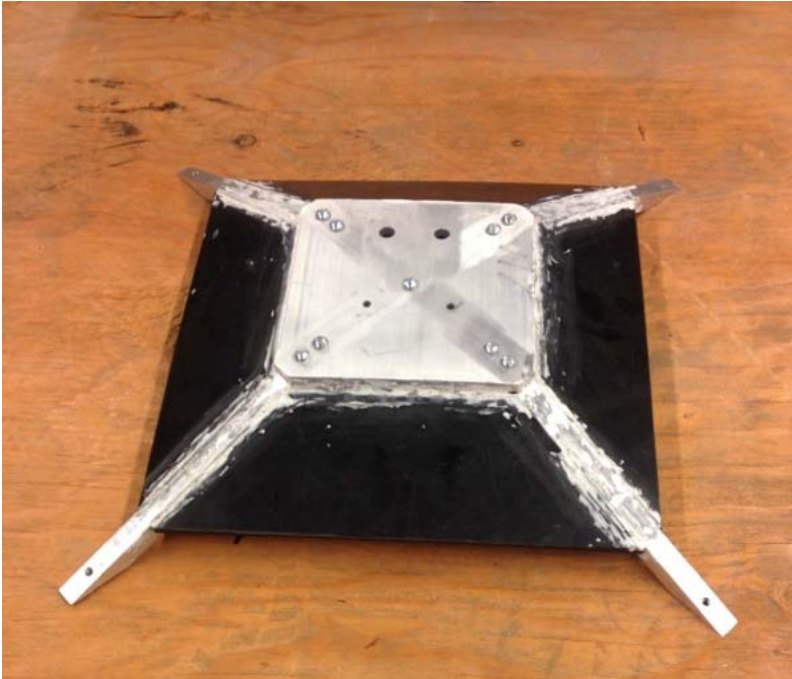
APPENDIX

A.1 – Assembly process

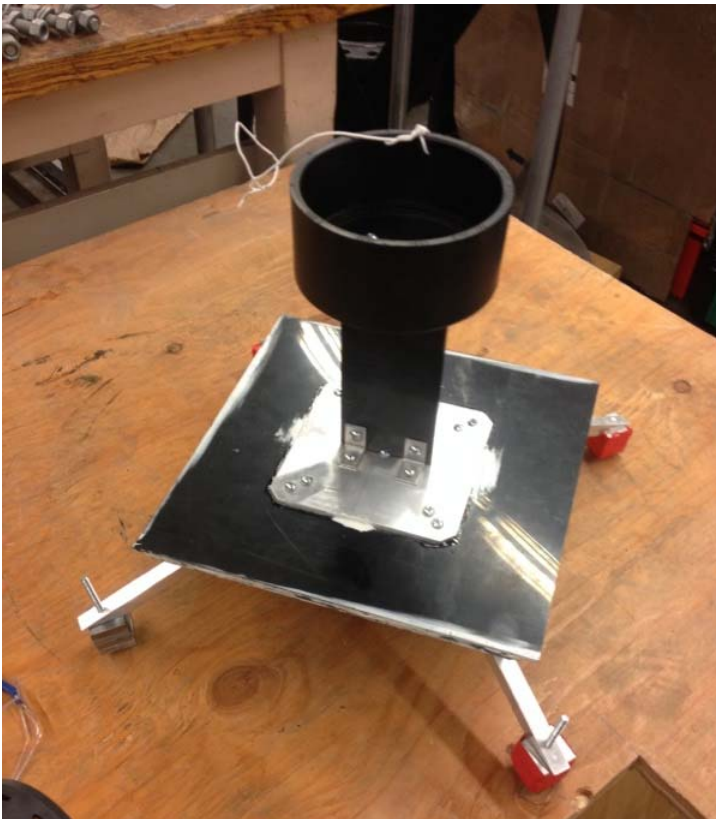


Bracing the inverted skirts in place while the epoxy sets

A.2 – Completed models



Finished scale model with standard skirt



Completed assembly of the inverted skirt model

A.3 - Static Test

As mentioned in the Test Results and Analysis section, a static tipping test was conducted ultimately to determine the maximum resisting moment of each model (ARM).

Our base model has relatively complex geometries, so rather than calculate the Center of Mass (COM) location analytically or using a sophisticated experimental procedure, a simple tipping test was conducted to determine its resisting moment. With the base model submerged, the model was pushed with a gram-accuracy scale into a horizontal acrylic rod at a known vertical distance from the tipping fulcrum. From the force required to tip and the vertical distance to the fulcrum, resisting moment of the model was directly calculated for the for 0, 5, and 9 degrees inclination (all were around 1 N-m, with 0 degrees inclination being about 10% higher than for 9 degrees). See Table 5 below for tipping test results.

Table - Static test results

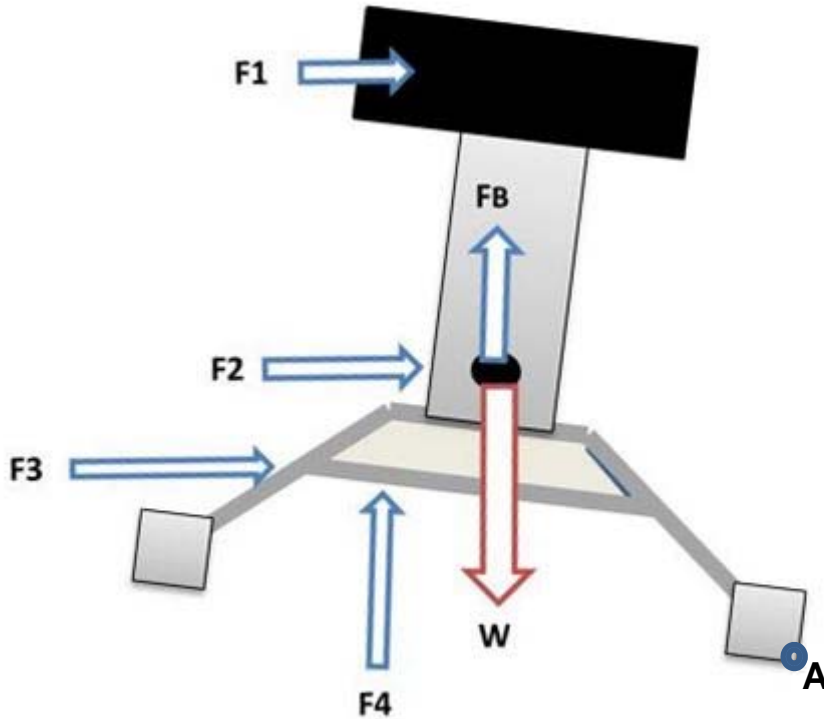
Angle (degrees)	Force at Onset of Tipping (N)	Moment Arm (cm)
0	2.23	45.7
5	2.08	47.1
9	2.02	47.9

A.4 - Components for UIIB

1. Buoy
2. Acoustic Doppler current profiler
3. Acoustic release
4. Line canisters
5. Water quality sensor: Seabird 16+ v2
6. Hydrophone: Loggerhead DSG
7. BioSonics DTX
8. Fish tag receiver: Vemco VR2W
9. Cetacean click detector: C-POD
10. SoundMetrics DIDSON

A.5 - Sample PTM Calculation (Test Case 2)

- Test Case 2 - Standard base at 7.5-degree incline ($\theta = 7.5$), shown below with F_{1-4} (defined in “definitions” section) acting at their respective points of action (POA)
- All 4 PTM calculations were done the same way, and in general for this project all overturning calculations were done the same way



Calculation Goal: To determine the total tipping moment that CFD and analytics together would predict (PTM) for Test Case 2 at the actual tipping velocity of 0.52 (m/s).

Definitions

$$\text{Predicted Tipping Moment (PTM)} = \sum M_A = F_1x_1 + F_2x_2 + F_3x_3 + F_4x_4$$

F_1 = net drag force on upper cylinder (calculated analytically)

F_2 = net drag force on turbine plate (calculated analytically)

F_3 = net drag force on base (calculated indirectly from CFD results)

F_4 = net lift force on base (calculated indirectly from CFD results)

x_1 = moment arm of F_1 = vertical distance from line of action of F_1 to A

$x_2 =$ moment arm of $F_2 =$ vertical distance from line of action of F_2 to A
 $x_3 =$ moment arm of $F_3 =$ vertical distance from line of action of F_3 to A
 $x_4 =$ moment arm of $F_4 =$ horizontal distance from line of action of F_4 to A

$$F_1 = \frac{1}{2} \rho v^2 C_{D_1} A_1$$

$$F_2 = \frac{1}{2} \rho v^2 C_{D_2} A_2$$

Assumptions – Lift and Drag Forces

General:

- F_{1-4} are the only forces tending to tip the model
- Water interacts with each component in the full model exactly as it would with each component totally isolated from the rest (i.e., no interaction between components)

For the determination of F_1 :

- $C_{D_1} A_1 =$ the same as at zero degrees incline: A_1 increases slightly with inclination because of exposure of the top and bottom of the cylinder, but C_{D_1} decreases slightly from the textbook value because flow is not perpendicular; therefore their product was assumed to be roughly equivalent to the product of A_1 and C_D in the case of zero degrees incline. (The frontal area could have been exactly determined from geometry, but without a revised value of C_D there is no significant improvement in accuracy; and a published value of C_D could not be located for such a case.)

$$F_1 = \frac{1}{2} \rho v^2 C_{D_1} A_1 = \frac{1}{2} (1025)(0.52)^2 (1.2)(0.127 \times 0.057) = 1.2 \text{ (N)}$$

For the determination of F_2 :

- $C_{D_2} A_2 =$ the same as at zero degrees incline: A_2 decreases from the non-inclined case according to $\cos 7.5 = 0.99$, (i.e, by a negligible amount); C_{D_2} probably decreases but also not by much and not in a way that could have been easily accounted for.

$$F_2 = \frac{1}{2} \rho v^2 C_{D_2} A_2 = \frac{1}{2} (1025)(0.52)^2 (1.98)(0.16 \times 0.073) = 3.1 \text{ (N)}$$

For the determination of F_3 :

- $F_3 \cong 4$ (N): A CFD analysis at 7.5 degrees; the drag force on the base from the CFD conducted at 5 degrees for this particular model was 3.3 N, and using the associated coefficient of drag and a new, larger area, and accounting for the blockage from the turbine plate which was not represented in the CFD, the new drag force was estimated (somewhat arbitrarily) to be approximately 4 N.

$$F_3 \cong 4 \text{ (N)}$$

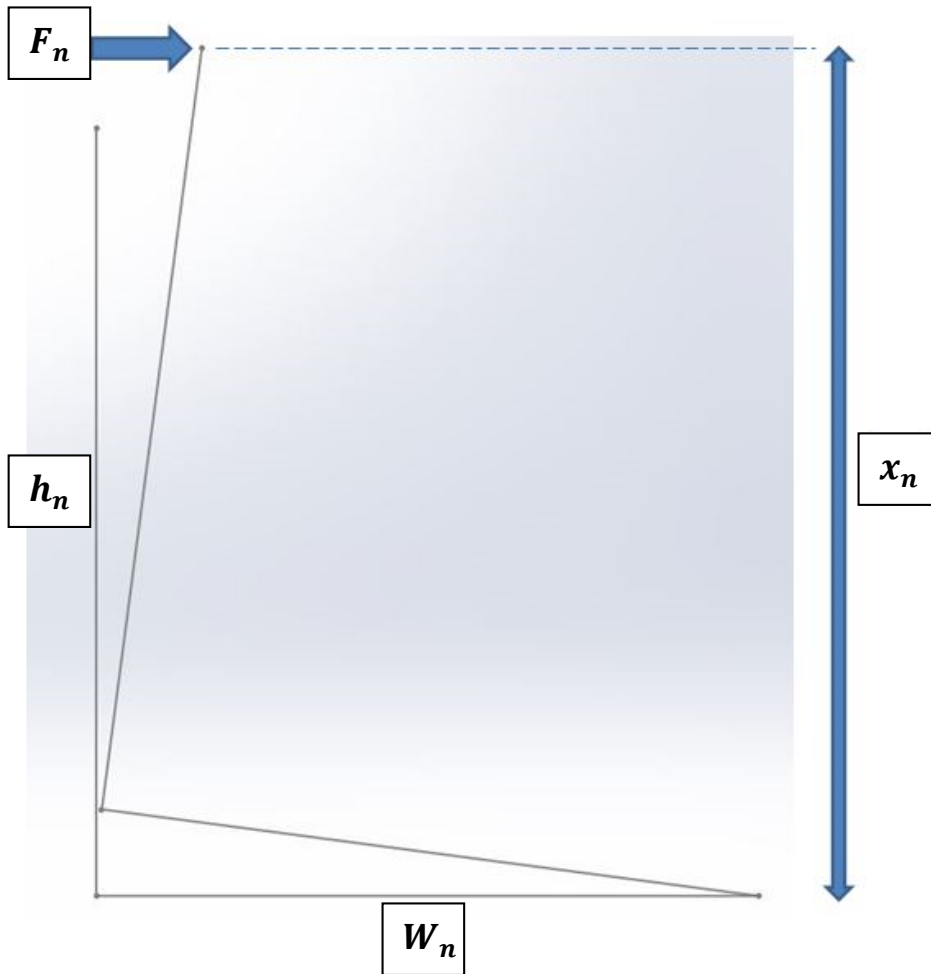
For the determination of F_4 :

- $F_4 \cong 4$ (N): The lift force on the base from the CFD was 5.1 N, again for the 5 degree case. According to several lift equations from a NASA website, the lift force would increase for a higher angle of inclination (to a point). Blockage from the turbine plate, unaccounted for in the CFD, would tend to lower the pressure above the base and thereby decrease lift. From intuition and certain CFD results, the magnitude of the second of these counteractive effects was assumed to be relatively larger, and accordingly it was estimated (again, somewhat arbitrarily) that the actual lift force to be somewhat lower, around 4 N. With more extensive CFD analysis we could determine F_3 and F_4 more accurately.

$$F_4 \cong 4 \text{ (N)}$$

Determination of Moment Arms

The moment arm of each force when the model is angled to 7.5 degrees depends not just on the vertical distance of the point of action of each force from the fulcrum, h_n but also on the horizontal distance, w_n . The h values were determined directly from the model in a straightforward way. The w values were somewhat more complicated to determine. For drag forces on perpendicular faces, the point of action (POA) of each resultant force was assumed to be at the geometric center of the face; for lift forces the POA was assumed to be at the center of pressure as determined from the CFD or from an analytical estimate; drag forces on the upper cylinder were assumed to act somewhat behind the front of the cylinder, near the COP.



n	w_n (m)	h_n (m)
1	0.24	0.28
2	0.18	0.17
3	0.32	0.057
4	0.25	0.070

$$x_1 = w_1 \sin \theta + h_1 \cos \theta = (0.24) \sin(7.5) + (0.28) \cos(7.5) = 0.31 \text{ (m)}$$

$$x_2 = w_2 \sin \theta + h_2 \cos \theta = (0.18) \sin(7.5) + (0.17) \cos(7.5) = 0.19 \text{ (m)}$$

$$x_3 = w_3 \sin \theta + h_3 \cos \theta = (0.32) \sin(7.5) + (0.057) \cos(7.5) = 0.10 \text{ (m)}$$

$$x_4 = h_4 \sin \theta + w_4 \cos \theta = (0.070) \sin(7.5) + (0.25) \cos(7.5) = 0.25 \text{ (m)}$$

$$PTM = F_1 x_1 + F_2 x_2 + F_3 x_3 + F_4 x_4 = (1.2)(0.31) + (3.1)(0.19) + (4)(0.10) + (4)(0.25) = 2.4 \text{ (N} \cdot \text{m)}$$